Monitoring Trapped Charge Generation for Gate Oxide Under Stress

Yung Hao Lin, Chung Len Lee, *Senior Member, IEEE,* and Tan Fu Lei

***Abstract*— A measurement method to extract the respective quantities and centroids of positive and negative trapped charges, i.e., Q_p and Q_n, generated by the negative current stress for gate oxides is proposed and demonstrated. The method is based on neutralization of Q_p by a low positive current stress to differentiate the effects of Q_p and Q_n. From the extracted quantities and centroids of Q_p and Q_n of negatively stressed oxides, it was found that Q_p and Q_n are generated near the oxide/substrate interface and Q_p is initially much larger than Q_n. After the continuous stressing, Q_p saturates and moves closer to the interface, but Q_n keeps increasing and moves away from the interface, especially for those oxides after the post-poly anneal (PPA) treatment. Q_p is very unstable and easily neutralized, either by a small stress of opposite polarity or the same polarity. For the latter, Q_p is mainly dependent on the level of the final stressing field.**

I. INTRODUCTION

HIGH field stresses are commonly used to evaluate the gate oxide reliability. The stress-induced trapped charges in the oxide film result in threshold voltage shifts, excess leakage currents and even oxide breakdowns. Previously, the distributions of trapped charges were measured and discussed to analyze trapping mechanisms [1]–[8]. However, in the stress, both positive (Q_p) and negative (Q_n) trapped charges are simultaneously generated [1]–[6]. In previous studies, effects of Q_p and Q_n were not differentiated and their net effects were measured when stress-induced $C-V$ or $I-V$ curve shifts were analyzed. To fully understand the trappings and the related degradation mechanisms of gate oxide films, it is desirable to monitor Q_p and Q_n generation, respectively, during the stress.

In this paper, a new method is proposed to monitor the distributions of Q_p and Q_n, respectively. Unlike Q_n, Q_p is very unstable and easy to be neutralized by a low reverse bias stress [6], [9]. Thus, the respective effects of Q_p and Q_n on $C-V$ and $I-V$ curve shifts were differentiated by neutralizing Q_p. Then their individual trapping quantities and centroids in the oxide film were extracted. Thus their dependence on stressing currents and injected charges under constant current stresses was monitored. Moreover, the relations between the oxide quality and the trapping characteristics were also studied by using the post-poly-annealing (PPA) method which was to degrade the oxide film [10]. In addition, the dynamic change of trapping distributions in the oxide film under different injection conditions were also studied. It was found that Q_p has a reversible characteristics, with its steady-state trapping level determined by the final oxide field [9], [11], and additional stresses only generate extra Q_n but does not disturb the original Q_n.

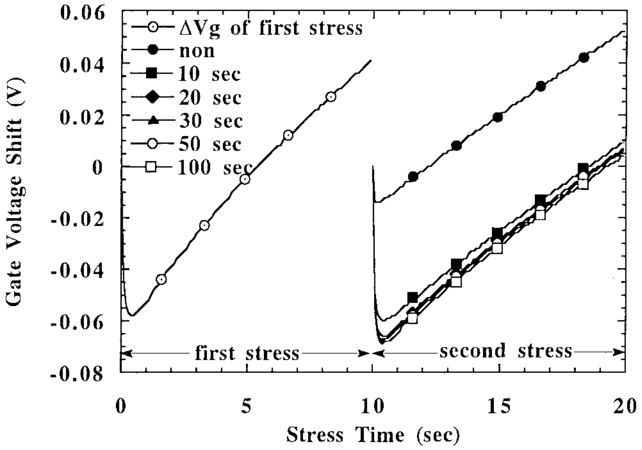

Fig. 1. The gate voltage shifts (ΔV_g) for samples under two consecutive -100 mA/cm^2 stresses. Between these two consecutive steps of negative stresses, small opposite $+0.1$ mA/cm^2 stresses were applied for different times (s) to neutralize the pregenerated Q_p in the oxide film.

II. EXPERIMENT TECHNIQUES

The samples used in this study were $POCl_3$-doped gate MOS capacitors, with an area of 2.33×10^{-4} cm^2, on a p-type Si wafer. The 80 Å gate oxide was grown in diluted dry O_2 ($O_2/N_2 = 1/6$) at 900 °C and annealed in N_2 at the same temperature for 15 min. The poly-Si gate was metallized with Al followed by a 400 °C anneal in N_2 for 30 min. For some samples, the gate oxides were degraded by the PPA, before $POCl_3$ doping, in N_2 at 900, 950, and 1000 °C, respectively, for 10 min. HP4145B and Keithley $C-V$ analyzer were used to measure sample electrical characteristics.

III. RESULTS AND DISCUSSIONS

As mentioned previously, both positive (Q_p) and negative (Q_n) trapped charges are generated during high field stresses [1]–[6], and Q_p is very unstable and easy to be neutralized by a low reverse bias stress [6], [9]. An experiment was done by applying two consecutive -100 mA/cm^2 stresses to a group of similar samples, but with some samples applied with small opposite $+0.1$ mA/cm^2 stresses for different times between these two consecutive stresses. The first and the second $-V_g$ stresses were both applied for 10 s. Fig. 1 shows

---

Manuscript received November 15, 1996; revised January 17, 1997. The review of this paper was arranged by Editor C.-Y. Lu. This work was supported by the National Science Council of R.O.C. under Research Contract NSC86-2215-E009-025.

The authors are with the Department of Electronics Engineering and Institute of Electronics, National Chiao-Tung University, Hsinchu 300, Taiwan, R.O.C.

Publisher Item Identifier S 0018-9383(97)06127-3.

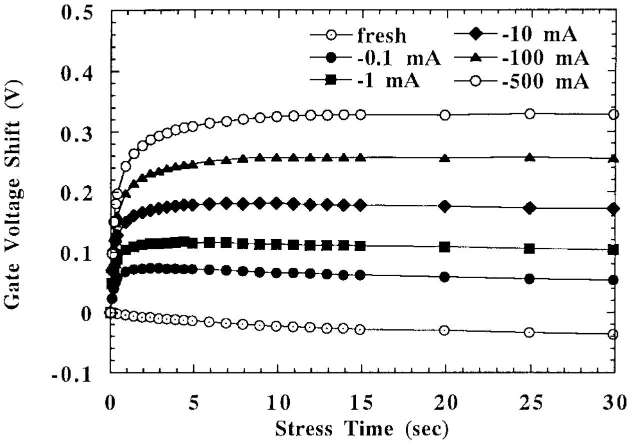

Fig. 2. The gate voltage shifts (ΔV_g) under $+0.1$ mA/cm^2 stress for samples prestressed by -0.1, -1, -10, -100, and -500 mA/cm^2 with the same total injected charges of -1 C/cm^2. The neutralization of $-J_g$ stress-generated Q_p by the $+J_g$ stresses led to the initial increase of their ΔV_g curves. The higher the $-J_g$, the larger the initial ΔV_g-increment, i.e., the more Q_p neutralized.

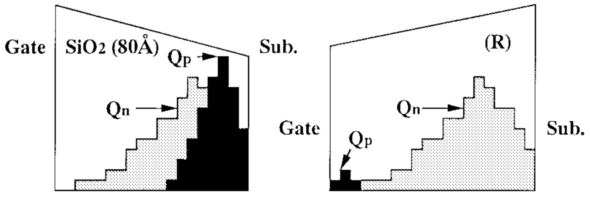

(a) (b)

Fig. 3. The distributions of Q_p and Q_n, pregenerated by a $-V_g$ stress, (a) before and (b) after application of the $+0.1$ mA/cm^2 stress. Q_p near the SiO$_2$/Si interface had been neutralized and small quantity of newly generated Q_p appeared near the gate/SiO$_2$ interface due to the small reverse positive stress but Q_n stayed undisturbed.

the gate voltage shifts (ΔV_g) of these samples. The first stress generated Q_p which caused the initial decrease of ΔV_g. The amount of generated Q_p then saturated [5] and then Q_n, which was generated at the same time, kept increasing. This caused ΔV_g to increase henceoff. During the second consecutive stress, the sample which did not receive the reverse $+0.1$ mA/cm^2 current stress had a constant increase in the ΔV_g curve. However, for the samples which did receive the reverse $+0.1$ mA/cm^2 current stress, the ΔV_g decreased at the very initial stress, just like that of the first stress. This indicates that the Q_p generated by the first negative stress was neutralized by the reverse $+0.1$ mA/cm^2 current stress and re-generated during the second stress. For these samples, it is also seen that the decrease in ΔV_g saturates after the $+0.1$ mA/cm^2 stress for 20 s. This suggests that the precreated Q_p had been completely neutralized. And in the following studies, a $+0.1$ mA/cm^2 stress for 30 s was applied to neutralize the negatively created Q_p and thus differentiate the respective effects of Q_p and Q_n.

Fig. 2 shows gate voltage shifts, ΔV_g, of $+0.1$ mA/cm^2 stresses for the samples to which negative stresses of different current densities had been preapplied, but with the same total injected charges of -1 C/cm^2. For the fresh sample, which did not receive any negative stresses, the ΔV_g curve decreased due to the generation of Q_p near the gate/SiO$_2$ interface [3]–[5], [8] upon $+J_g$ stressing. However, for the samples which had been prestressed with negative currents, all ΔV_g curves increased rapidly initially then saturated. These initial voltage increments were resulted from recombination of the positively injected electrons with the preexisting Q_p's which were generated by the negative prestressing currents. The more Q_p's generated by the higher negative current stress [7]–[9], the more the initial rising of the ΔV_g curve. The final saturation of all curves indicated that for all cases, Q_p had been completely neutralized by the positive current stress. On the other hand, since the positive neutralizing stress was relatively small, only $+0.1$ mA/cm^2 stress with 0.003 C/cm^2 of total injected charges, it is reasonable to assume that the distribution of the preexisting Q_n was not disturbed by it.

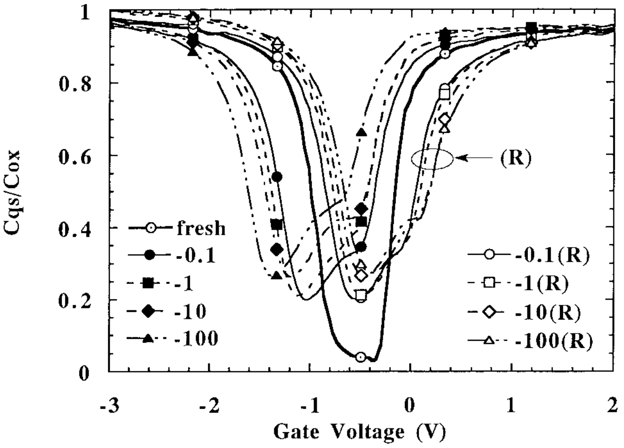

Fig. 4. The shifts of quasi-static $C-V$ curves after the $+J_g$ neutralizing stresses applied for samples prestressed with different $-J_g$ (mA/cm^2) stresses with the same total injected charges of -1 C/cm^2. The curves labeled with (R) were for samples neutralized.

The above phenomenon can be explained with the aid of Fig. 3, in which Fig. 3(a) shows the generated Q_p and Q_n after the first negative stress, and Fig. 3(b) shows that Q_p near the SiO$_2$/Si interface had been neutralized and small quantity of newly generated Q_p appeared near the gate/SiO$_2$ interface due to the small reverse positive stress, but Q_n stayed undisturbed.

The above phenomenon is also reflected by $C-V$ and $I-V$ curves of the samples, measured before and after they were stressed and neutralized. Figs. 4 and 5 show the measured quasi-static $C-V$ and negative $I-V$ curves, respectively, of those samples. In these figures, the curves marked with (R) correspond to the samples which had been neutralized by the $+0.1$ mA/cm^2 stress. In Fig. 4, it can be seen that the $C-V$ curves of the negatively stressed samples shifted left with the -100 mA/cm^2 shifting most. This indicates that Q_p was generated by negative stresses, where the amount of Q_p increased with increasing the stressing current. After the neutralizing $+0.1$ mA/cm^2 stress was applied, all the neutralized curves shifted right, indicating that Q_p's had been neutralized and the remaining originally generated Q_n shifted the $C-V$ curves to the right. Comparing these two groups of curves, we find that they are the same in the shape, indicating that no new SiO$_2$/Si interface states were generated during the Q_p-neutralization process by the $+0.1$ mA/cm^2 injection. In Fig. 5, all the negatively stressed $I-V$ curves also shifted

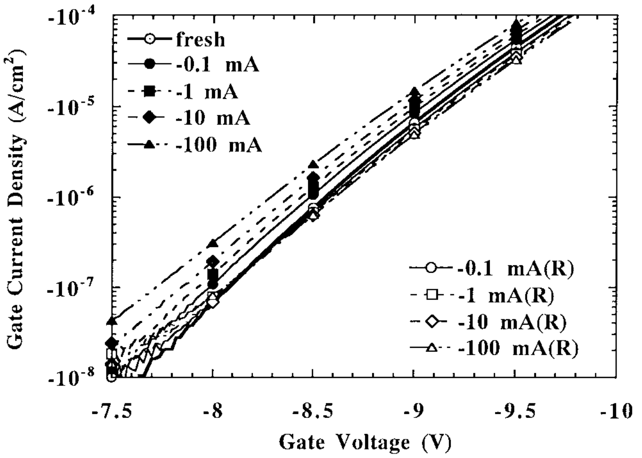

Fig. 5. The shifts of negative $I{-}V$ curves after the $+J_g$ neutralizing stresses applied for samples prestressed with different $-J_g$ (mA/cm^2) stresses with the same total injected charges of -1 C/cm^2. The curves labeled with (R) were for samples neutralized.

left with the -100 mA/cm^2-stressed curve shifting most. After the Q_p-neutralization, all curves shifted right. This exhibits the same results of the $C{-}V$ curves.

From the shifts of the above $C{-}V$ and $I{-}V$ curves, before and after Q_p-neutralization, we can derive the quantities and locations of centroids for Q_p and Q_n, respectively. This can be done in the following way: Comparing the $C{-}V$ curves of a sample, before and after its Q_p-neutralization, we can derive the flat band difference (ΔV_{fb}) of these two curves. Similarly, we can derive the gate voltage shift $(\Delta V_{g,-\text{IV}})$ of the negative $I{-}V$ curves of the sample, before and after it was neutralized. During measuring this $\Delta V_{g,-\text{IV}}$, the $I{-}V$ curves were measured at a current level of -10^{-6} A/cm^2 to prevent disturbing the unstable Q_p in oxide film. The obtained ΔV_{fb} and $\Delta V_{g,-\text{IV}}$, mainly due to the existence and nonexistence of Q_p, can be used to be ΔV_{p+} and ΔV_{p-}, respectively, in the following equations to compute the quantity and the location of Q_p [12]

$$Q_{p(n)} = -\varepsilon_{\text{ox}} * (\Delta V_{p(n)+} + \Delta V_{p(n)-})/T_{\text{ox}} \qquad \text{(1a)}$$

$$d_{p(n)} = T_{\text{ox}} * \Delta V_{p(n)-}/(\Delta V_{p(n)+} + \Delta V_{p(n)-}) \qquad \text{(1b)}$$

where $d_{p(n)}$, ε_{ox}, and T_{ox} are the centroid of $Q_{p(n)}$ measured from the substrate, the oxide dielectric constant and the oxide thickness, respectively.

On the other hand, after the Q_p-neutralization, nearly only Q_n existed in the oxide film. We can also derive the quantity and the centroid of Q_n by computing ΔV_{n+} and ΔV_{n-} from the curves of Figs. 4 and 5. In these figures, the curves marked with (R) are curves corresponding to the case where only Q_n is present in the oxide film. And comparing the (R) curves with the curve of the fresh sample, we can derive ΔV_{fb} and $\Delta V_{g,-\text{IV}}$, which are used to be ΔV_{n+} and ΔV_{n-}, respectively. In this case, $\Delta V_{g,-\text{IV}}$ was extracted at a current level of -10^{-4} A/cm^2 to minimize the amount of undetectable charges trapped in the tunneling distance of negative $I{-}V$ measurement. With the obtained ΔV_{n+} and ΔV_{n-}, the quantity and the location of the centroid of Q_n can be computed by using the similar formulas of (1).

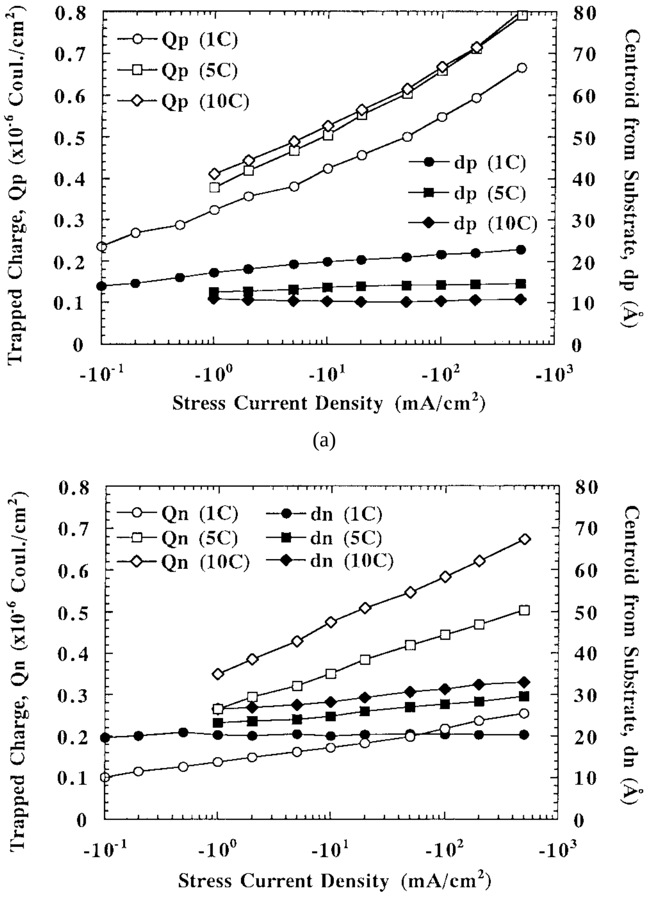

(a)

(b)

Fig. 6. The calculated quantities $(Q_{p(n)})$ and centroids $(d_{p(n)})$ of both (a) positive and (b) negative trapped charges generated by different negative current stresses with -1, -5, and -10 C/cm^2 of total charges injected. Larger Q_p and Q_n are generated for higher current stresses, and both charges are trapped near the anode.

It has to be mentioned that the above method can only be applied to monitor distributions of trapped charges generated by negative gate voltage stresses. This is because the trapped charges are mostly generated near the SiO$_2$/Si interface [3]–[5], [8] under the $-V_g$ stress. They can be detected by the $C{-}V$ and the negative $I{-}V$ curve shifts. However, for the positive stress, the generated charges are mostly near the gate/SiO$_2$ interface. The $C{-}V$ curves and negative $I{-}V$ curves are not sensitive to their existence. And thus the positively created charges can not be fully and correctly detected by our method. This is also the reason that, in Fig. 3(b), although a comparatively small quantity of Q_p were unavoidably generated near the gate/SiO$_2$ interface during the $+0.1$ mA/cm^2 neutralizing stress, they were neglected in the previous computation for determining Q_p and Q_n. Moreover, for the positive stress, an opposite -0.1 mA/cm^2 stress is needed to neutralize the precreated Q_p. This -0.1 mA/cm^2 stress will also inevitably generate new Q_p near the SiO$_2$/Si interface. And this can not be neglected as in the negative stress case, since errors will be introduced in the extracted data.

The above method was used to extract the quantities and locations of the centroids of generated Q_p and Q_n in the oxide stressed by different negative current densities. Fig. 6(a) and (b) shows the extracted data for Q_p and Q_n,

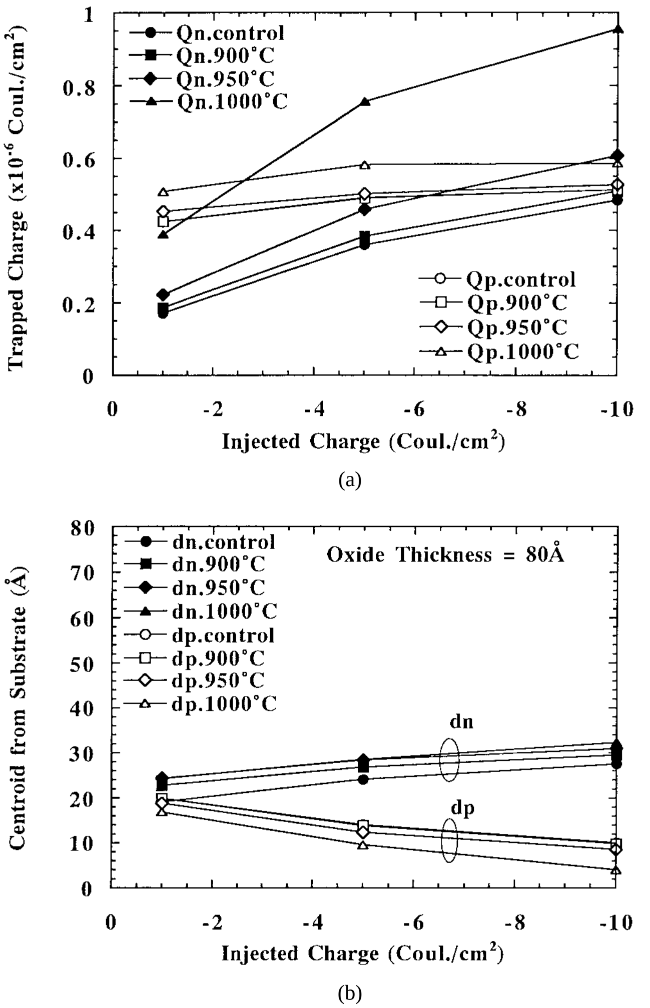

(a)

(b)

Fig. 7. The calculated (a) quantities ($Q_{p(n)}$) and (b) centroids ($d_{p(n)}$) of both positive and negative trapped charges generated by -10 mA/cm^2 stresses with -1, -5, and -10 C/cm^2 of total injected charges. In which, oxides of some samples were degraded by the PPA at 900, 950, or 1000 °C for 10 min.

respectively, for the total stressing charges of -1, -5, and -10 C/cm^2. Both generated trapped charges are found to be near the anode [3]–[5], [8], while the higher the stressing current density, the more away the centroid is from the substrate, in addition to the larger generated quantities [7]–[9]. This is easy to be understood since the higher current density needs a higher applied field which gives more energy to injected electrons to generate traps in the oxide. On the other hand, Q_p increases rapidly at the initial stress and is larger than Q_n for this range of stressing current. While when increasing the injected charges, Q_p saturates after the injected charges reaches 5 C [5], but Q_n keeps increasing. This suggests that, initially in the oxide, hole traps are much more than electron traps. Upon stressing, these hole traps are easily filled up, which depends on the stressing field, and afterward electron traps are continuously generated by the stressing current.

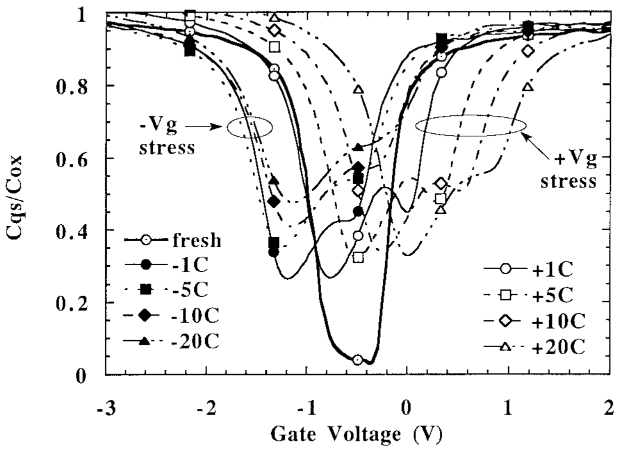

Fig. 8. The changes of quasi-static C–V curves after $+10$ or -10 mA/cm^2 stresses, both with the total injected charges of 1, 5, 10, and 20 C/cm^2.

The above method was also used to investigate the reliability of oxides for the samples subjected to post-poly-annealing (PPA) at 900, 950, and 1000 °C, respectively, by monitoring the stress generated charges. Fig. 7(a) and (b) shows the quantities of Q_p and Q_n, and their respective centroids, d_p and d_n, of the samples stressed by -10 mA/cm^2 with -1, -5, and -10 C/cm^2 of total injected charges. These figures show that more Q_p and Q_n are generated for the samples applied by PPA at the higher temperature [10], and Q_n is more susceptible to the PPA. This indicates that PPA does degrade the quality of the oxide and the factor to cause oxide breakdown is mainly associated with the Q_n generation. Also, for the higher PPA temperature or the larger injected charges, the centroid of Q_n is more far away from the substrate, i.e. more near the injection interface. This also indicates that a shorter accelerating distance is sufficient for the injected electrons to generate Q_n trapping states in the degraded oxide which probably has more weak spots in it after PPA. But for Q_p, the trend is opposite. In which, its centroid, d_p, becomes closer to the substrate for the higher PPA temperature or the larger injected charges.

As mentioned previously, Q_p and Q_n of $+V_g$ stressed oxides can not be derived by our proposed method. It is interesting also to investigate these trapped charge distributions in the oxide. Fig. 8 shows the changes of normalized quasi-static C–V curves ($C_{\rm qs}/C_{\rm ox}$) for MOS capacitors after they were stressed by -10 or $+10$ mA/cm^2, both with 1, 5, 10, and 20 C/cm^2 of total charges injected. The larger distortions of negatively stressed curves reveal that the interface states generated by $-V_g$ stress were more than those by $+V_g$ stress, especially for large injected charges. This could be attributed to that, upon $-V_g$ stressing, electrons were injected from the gate and thus more damages were created at the oxide/substrate interface to generate interface states [13]. On the other hand, at the initial stage of $-V_g$ stresses, i.e., the -1 C and -5 C stresses, the curves shifted to the negative due to a large amount of Q_p generated near the oxide/substrate interface. When increasing the injected charges, Q_p remained almost constant and Q_n was continuously generated. But the effect of Q_n was not felt in the curves' shifts, since d_p, the centroid of Q_p, moved closer while d_n moved away from the oxide/substrate interface. However, for the $+V_g$ stresses, the more the stress, the more the curves shifted to the positive. This probably indicates that Q_p and Q_n were generated near the gate/oxide interface with their centroids,

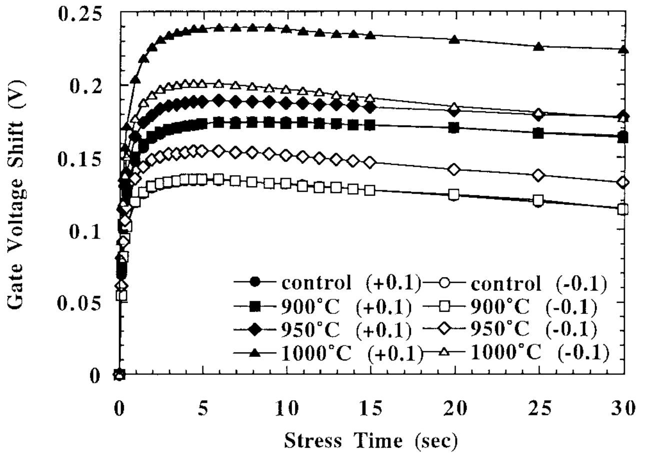

Fig. 9. The gate voltage shifts (ΔV_g) under $+0.1(-0.1)$ mA/cm^2 stresses, which were used to neutralize Q_p in oxide films, for samples prestressed by $-10(+10)$ mA/cm^2 with $-1(+1)$ C/cm^2 of total injected charges. In which, oxides of some samples were degraded by the post-poly-annealing at 900, 950, or 1000 °C for 10 min.

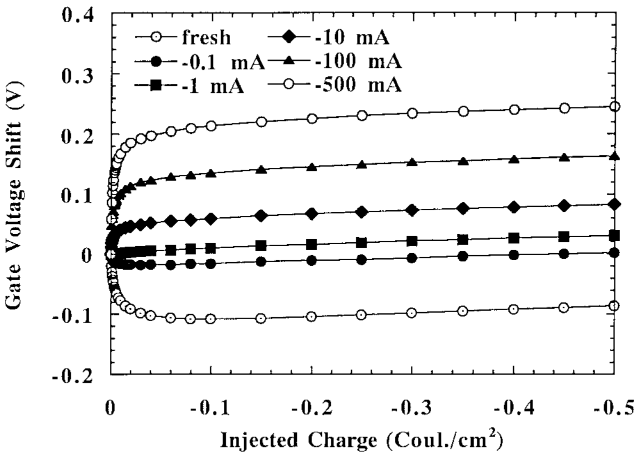

Fig. 10. The gate voltage shifts (ΔV_g) under $J_2 = -0.1$ mA/cm^2 stresses for samples prestressed by $J_1 = -0.1, -1, -10, -100,$ and -500 mA/cm^2 and all with -0.5 C/cm^2 of total injected charges. The larger the J_1 stress, the larger the initial ΔV_g-increment, i.e., the more excess pregenerated Q_p neutralized.

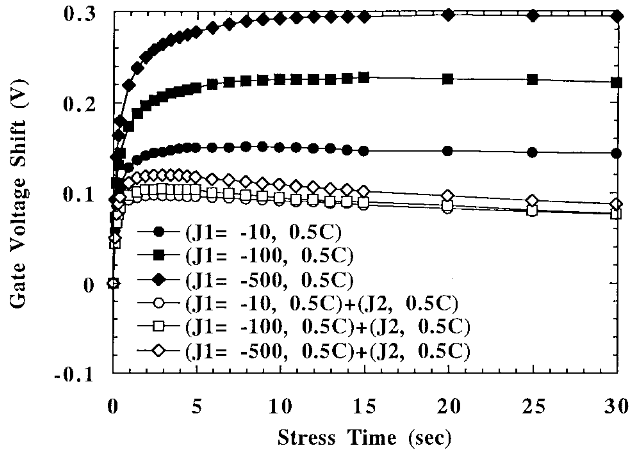

Fig. 11. The gate voltage shifts (ΔV_g) under the neutralizing $+0.1$ mA/cm^2 stresses for samples prestressed first by $J_1 = -10, -100,$ and -500 mA/cm^2 and then by $J_2 = -0.1$ mA/cm^2 (open dot curves), or only prestressed by J_1 (black dot curves), all with -0.5 C/cm^2 of total injected charges. The reductions of the initial ΔV_g-increments for samples with an additional J_2 stress imply that some J_1 stress-created Q_p were preneutralized.

d_p and d_n, shifting to the gate/oxide and the oxide/substrate interfaces, respectively. Moreover, the ΔV_g curves during the neutralization process by applying an opposite small stress can also give some hint on the quantity of positively generated Q_p. Fig. 9 shows the gate voltage shifts of -0.1 mA/cm^2 neutralizing stresses (in open dot curves) for the PPA treated samples which were prestressed by $+10$ mA/cm^2 with 1 C/cm^2 of total injected charges. The initial rapid increase of the curves indicate that $+V_g$ stress created Q_p was neutralized by the latter $-J_g$ stress. And the higher temperature PPA, the more Q_p's were generated upon $+V_g$ stressing. For comparison, similar samples were applied with -10 mA/cm^2 stress but neutralized by $+0.1$ mA/cm^2, and their ΔV_g curves corresponding to this $+0.1$ mA/cm^2 neutralizing stress are also plotted in Fig. 9 (in black dot curves). Comparing the initial increments of these ΔV_g curves, we find that the $+V_g$ stressed curves have smaller initial increments than those of $-V_g$ stressed curves, i.e., Q_p generated by $+V_g$ stress is less than that of $-V_g$ stress. This may also be one of the reasons for that $-V_g$ stresses result in smaller breakdown charges than $+V_g$ stresses [14].

In the end of this work, the reversible characteristics of trapped charges, with their trapping levels being irrespective to the previous stresses but only determined by the final stressing field [9], [11], is investigated. In this study, samples were first stressed by a J_1 of different densities of -500, -100, -10, -1, and -0.1 mA/cm^2, all with -0.5 C/cm^2 of total injected charges, to generate trapped charges in the oxides. Then they were stressed again by a following second J_2 of -0.1 mA/cm^2 stress. During this J_2 stress, the gate voltage shifts, ΔV_g, were plotted in Fig. 10. For fresh sample, which was not J_1 stressed, the initial decrease of its ΔV_g curve indicates that Q_p was generated upon J_2 stressing. However, the other samples with J_1 prestresses have initial increments on their ΔV_g curves, indicating Q_p's generated in the first J_1 prestressing step were neutralized by the following J_2 stress. Also for the samples with higher J_1 stresses, the larger initial increments are observed. It is because the magnitude of the following J_2 stress was comparatively smaller than that of J_1 (-1 mA to -500 mA, except -0.1 mA) and hence J_2 did not generate Q_p, instead, neutralized the J_1 pregenerated Q_p near the oxide/substrate interface. This can be further verified by observing the ΔV_g curves of the samples applied with a $+0.1$ mA/cm^2 stress to neutralize the remaining Q_p's after the J_2 stress. The ΔV_g curves are shown in Fig. 11 (in open dot curves). For comparison, the ΔV_g curves of $+0.1$ mA/cm^2 neutralizing stresses for another similar set of samples, which were not applied with the J_2 stress to neutralize the J_1 stress created Q_p's, are also shown in Fig. 11 (in black dot curves). The black dot curves have much larger initial increments, especially for the higher J_1 stress, indicating more Q_p's were neutralized by the $+0.1$ mA/cm^2 stress. On the contrary, the three open dot curves have much smaller initial increments and almost coincide together. This again verifies that a large portion of Q_p had already been neutralized by the J_2 stress.

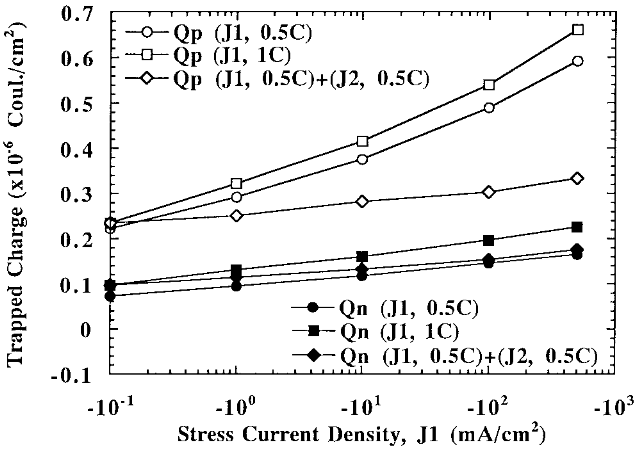

Fig. 12. The calculated quantities of both Q_p (open dot curves) and Q_n (black dot curves) for samples after they were just J_1 stressed (circular and square dot curves for the total injected charges of 0.5 C and 1 C, respectively), and then $J_2 = -0.1$ mA/cm^2 neutralized (diamond dot curves for the total injected charges for J_1 of 0.5 C followed by J_2 of 0.5 C).

The quantities of Q_p and Q_n of the above samples after they were just J_1 stressed and then J_2 neutralized, respectively, were also extracted by using our proposed method. Fig. 12 shows the extracted quantities of Q_p and Q_n for the above samples. It can be seen that just after J_1 stresses (the circular dot curves of total injected charge of 0.5 C and the square dot curves of total injected charge of 1 C), the higher J_1 stressing current or the larger injected charges resulted in the larger Q_p and Q_n. However, when the J_2 stress was applied (the diamond dot curves of the total injected charges for J_1 of 0.5 C followed by J_2 of 0.5 C), the pregenerated Q_p is found to decrease, especially for higher J_1 current densities. And the resulted Q_p's for all J_1 densities are very close in their quantities. This indicates that Q_p's generated by J_1 stresses were neutralized by J_2 and their final quantities depend somehow on the level of the final J_2 stressing current. That is, Q_p is irrespective to the previous stresses but only determined by the final stressing field. On the other hand, Q_n keeps increasing for the additional J_2 stress. This also indicates that precreated Q_n, not like Q_p, is very stable and not easy to be disturbed by the following stress.

IV. CONCLUSION

In this paper, a measurement method was proposed to monitor the respective quantity and centroid of charges, Q_p and Q_n, which were generated by the negatively applied high field stress. The method was based on the Q_p-neutralization by a low positive current stress to differentiate the effects of Q_p and Q_n on $C{-}V$ and $I{-}V$ curves. By using this method to extract the quantities and centroids of Q_p and Q_n, we found that Q_p and Q_n are generated near the oxide/substrate interface by the negative stress. And higher fields or more injected charges generate larger quantities of Q_p and Q_n. During stressing, Q_p is initially much larger than Q_n, but then Q_p saturates in its quantity and moves closer to the oxide/substrate interface, while Q_n keeps increasing and moves away from the interface, especially for those PPA treated oxides. Q_p is very unstable and easy to be neutralized, either by a small stress of opposite polarity or the same polarity. For the latter, it is the so called "reversible characteristics" of Q_p, i.e., the quantity of Q_p is mainly dependent on the level of the final stressing field.

REFERENCES

[1] D. J. DiMaria, D. Arnold, and E. Cartier, "Impact ionization and positive charge formation in silicon dioxide films on silicon," *Appl. Phys. Lett.*, vol. 60, p. 2118, 1992.

[2] D. J. DiMaria, "Hole trapping, substrate currents, and breakdown in thin silicon dioxide films," *IEEE Electron Device Lett.*, vol. 16, p. 184, 1995.

[3] D. J. DiMaria and J. W. Stasiak, "Trap creation in silicon dioxide produced by hot electrons," *J. Appl. Phys.*, vol. 65, p. 2342, 1989.

[4] M. M. Heyns, R. F. DeKeersmaecker, and M. W. Hillen, "Trap generation and electron detrapping in SiO$_2$ during high-field stressing of metal-oxide-semiconductor structures," *Appl. Phys. Lett.*, vol. 44, p. 202, 1984.

[5] M.-S. Liang, C. Chang, Y. T. Yeow, and C. Hu, "MOSFET degradation due to stressing of thin oxide," *IEEE Trans. Electron Devices*, vol. ED-31, p. 1238, 1984.

[6] C. S. Jeng, T. R. Ranganath, C. H. Huang, H. S. Jones, and T. T. L. Chang, "High-field generation of electron traps and charge trapping in ultra-thin SiO$_2$," in *IEDM Tech. Dig.*, 1981, p. 388.

[7] Y. Nissan-Cohen, J. Shappir, and D. Frohman-Bentchkowsky, "Determination of SiO$_2$ trapped charge distribution by capacitance-voltage analysis of undoped polycrystalline silicon-oxide-silicon capacitors," *Appl. Phys. Lett.*, vol. 44, p. 417, 1984.

[8] ——, "High-field and current-induced positive charge in thermal SiO$_2$ layers," *J. Appl. Phys.*, vol. 57, p. 2830, 1985.

[9] Y. Nissan-Cohen, J. Shappir, and D. Frohman-Bentchkowsky, "High field current induced-positive charge transients in SiO$_2$," *J. Appl. Phys.*, vol. 54, p. 5793, 1983.

[10] R. Mehta, A. B. Bhattacharyya, and D. N. Singh, "Post-growth process-induced degradation in thin gate oxides," *J. Appl. Phys.*, vol. 69, no. 12, p. 8247, 1991.

[11] Y. Nissan-Cohen, J. Shappir, and D. Frohman-Bentchkowsky, "Dynamic model of trapping-detrapping in SiO$_2$," *J. Appl. Phys.*, vol. 58, p. 2252, 1985.

[12] D. J. DiMaria, "Determination of insulator bulk trapped charge densities and centroids from photocurrent-voltage characteristics of MOS structures," *J. Appl. Phys.*, vol. 47, p. 4073, 1976.

[13] P. P. Apte and K. C. Saraswat, "SiO$_2$ degradation with charge injection polarity," *IEEE Electron Device Lett.*, vol. 14, p. 512, 1993.

[14] Y. Hokari, "Stress voltage polarity dependence of thermally grown thin gate oxide wearout," *IEEE Trans. Electron Devices*, vol. 35, p. 1299, 1988.

Yung Hao Lin was born in Taichung, Taiwan, R.O.C., in 1969. He received the B.S. and Ph.D. degrees from the Department of Electronics Engineering, National Chiao-Tung University, Hsinchu, Taiwan, in 1991 and 1996, respectively. He is currently continuing postdoctoral research at National Chiao-Tung University. His research interests include the fabrication technology and the reliability analysis of thin gate dielectrics.

Chung Len Lee (S'70–M'75–SM'92), for a photograph and biography, see p. 159 of the January 1997 issue of this TRANSACTIONS.

Tan Fu Lei, for a photograph and biography, see p. 159 of the January 1997 issue of this TRANSACTIONS.